# A Neural Network Approach to Efficient Valuation of Large Portfolios of Variable Annuities

Seyed Amir Hejazi[a], Kenneth R. Jackson[a]

[a]*Department of Computer Science, University of Toronto, Toronto, ON, M5S 3G4, Canada*

**Abstract**

Managing and hedging the risks associated with Variable Annuity (VA) products require intraday valuation of key risk metrics for these products. The complex structure of VA products and computational complexity of their accurate evaluation have compelled insurance companies to adopt Monte Carlo (MC) simulations to value their large portfolios of VA products. Because the MC simulations are computationally demanding, especially for intraday valuations, insurance companies need more efficient valuation techniques. Recently, a framework based on traditional spatial interpolation techniques has been proposed that can significantly decrease the computational complexity of MC simulation (Gan and Lin, 2015). However, traditional interpolation techniques require the definition of a distance function that can significantly impact their accuracy. Moreover, none of the traditional spatial interpolation techniques provide all of the key properties of accuracy, efficiency, and granularity (Hejazi et al., 2015). In this paper, we present a neural network approach for the spatial interpolation framework that affords an efficient way to find an effective distance function. The proposed approach is accurate, efficient, and provides an accurate granular view of the input portfolio. Our numerical experiments illustrate the superiority of the performance of the proposed neural network approach compared to the traditional spatial interpolation schemes.

*Keywords:* Variable annuity, Spatial interpolation, Neural Network, Portfolio valuation

*Email addresses:* `amir@cs.toronto.edu` (Seyed Amir Hejazi), `krj@cs.toronto.edu` (Kenneth R. Jackson)

## 1. Introduction

A Variable Annuity (VA), also known as a segregated fund in Canada, is a type of mutual fund that comes with insurance features and guarantees. VAs allow policyholders to invest in financial markets by making payment(s) into a predefined set of sub-accounts set up by insurance companies and enjoy tax-sheltered growth on their investment. The insurer, later, returns these investments through a lump-sum payment or a series of contractually agreed upon payments. An attractive feature of VA products are the embedded guarantees that protect the investment of policyholders from downside market fluctuations in a bear market and mortality risks (TGA, 2013; Chi and Lin, 2012). For a detailed description of VA products and different types of guarantees offered in these products, see our earlier paper (Hejazi et al., 2015) and the references therein.

The innovative structure of embedded guarantees has made VA products a huge success. Major insurance companies, especially in the past decade, have sold trillions of dollars worth of these products (IRI, 2011), and have built up large portfolios of VA contracts, each with hundreds of thousands of contracts. The embedded guarantees of VA contracts in these portfolios expose insurance companies to a substantial amount of risk, such as market risk and behavioral risk. After the market crash of 2008 that wiped out several big insurance companies, the surviving insurance companies started major risk management initiatives to dynamically hedge (Hardy, 2003) their exposures.

An integral part of the aforementioned hedging programs is intraday evaluation of VA products to find the Greeks (Hull, 2006) for the portfolios of VA products so that effective hedging positions can be set up. Most of the academic methodologies for valuation of VA contracts are tailored to a specific type of VA contract (Milevsky and Salisbury, 2006; Chen and Forsyth, 2008; Chen et al., 2008; Dai et al., 2008; Ulm, 2006; Huang and Forsyth, 2011; Belanger et al., 2009) and/or are computationally too expensive to scale to large portfolios of VA contracts (Azimzadeh and Forsyth, 2015; Moenig and Bauer, 2011; Boyle and Tian, 2008). Hence, in practice, insurance companies have relied on nested MC simulations to find the Greeks of VA portfolios (Reynolds and Man, 2008). Nested MC simulations, as shown in Figure 1, consist of outer loop scenarios which span the space of key market variables and inner loop scenarios consisting of a collection of risk-neutral paths that are used to project the liabilities of VA contracts (Fox, 2013). Although MC
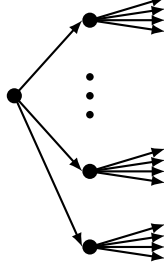
Figure 1: Pictorial graph of nested MC simulations.

simulations are computationally less expensive than the academic method-ologies, the amount of computation is still significant and does not scale well to large portfolios of VA contracts. Because of this, insurance companies are actively looking for ways to reduce the number of required MC simulations to find the Greeks for a large portfolio of VA contracts.

As we discuss in Section 2, a framework based on spatial interpolation (Burrough et al., 1998) has been successful in ameliorating the computa-tional load of MC simulations by reducing the number of VA contracts that go through nested MC simulation. However, as we discussed in (Hejazi et al., 2015), the proposed spatial interpolation framework requires an ef-fective choice of distance function and a sample of VA contracts from the space in which the input portfolio is defined to achieve an acceptable accu-racy level. The appropriate choice of the distance function for the given input portfolio in the proposed framework requires research by a subject matter expert for the given input portfolio. In this paper, we propose to replace the conventional spatial interpolation techniques– Kriging, Inverse Distance Weighting (IDW) and Radial Basis Function (RBF) (Burrough et al., 1998)– in the framework of (Hejazi et al., 2015) with a neural network. The pro-posed neural network can learn a good choice of distance function and use the given distance function to efficiently and accurately interpolate the Greeks for the input portfolio of VA contracts. The proposed neural network only requires knowledge of a set of parameters that can fully describe the types of VA contracts in the input portfolio and uses these parameters to find a good choice of distance function.

The rest of this paper is organized as follows. Section 2 provides a brief summary of existing methods for the valuation of portfolios of VA products. The main focus of Section 2 is on the spatial interpolation framework of (Hejazi et al., 2015) that has been successful in providing the Greeks for

3

a large portfolio of VA products in an efficient and accurate way. Section 3 describes the neural network framework and provides background information on neural networks. We provide the intuition behind the proposed model and the novel training technique used to calibrate (a.k.a. to train) the network. Section 4 provides insights into the performance of the neural network framework in estimation of Greeks for a large synthetic portfolio of VA contracts. Section 5 concludes the paper with a discussion of our future work and possible applications of the proposed framework.

## 2. Portfolio Valuation Techniques

If one thinks of VAs as exotic market instruments (Hull, 2006), the traditional replicating portfolio approach can be used to find the value of a portfolio of VA products. The main idea behind this approach is to approximate the cash flow of liabilities for a portfolio of VA contracts using well-formulated market instruments such as vanilla derivatives. The problem is often formulated as a convex optimization problem where the objective is to minimize the difference between the cash flow of the input portfolio and the replicating portfolio. Depending on the norm associated with the problem, linear programming (Dembo and Rosen, 1999) or quadratic programming (Daul and Vidal, 2009; Oechslin et al., 2007) is used in the literature to find the replicating portfolio. The replicating portfolio, in our application of interest, doesn't provide us with an efficient alternative to MC simulations, as one still needs to find the cash flow of the input portfolio for each year up to maturity.

Least Squares Monte Carlo (LSMC) regresses the liability of the input portfolio against some basis functions representing key economic factors (Longstaff and Schwartz, 2001; Carriere, 1996). LSMC has been proposed in the literature to reduce the number of inner loop scenarios in nested MC simulations (Cathcart and Morrison, 2009). Depending on the type of embedded guarantees, size of investment and characteristics of the policyholder, VA contracts have a significant number of numeric attributes, each covering a broad range. Therefore, an accurate regression using LSMC requires incorporation of many sample points, and hence is computationally demanding.

Recently, Replicated Stratified Sampling (RSS) (Vadiveloo, 2011) and Kriging based techniques (Gan, 2013; Gan and Lin, 2015) have been proposed to reduce the number of VA contracts that must be included in the MC simulations. Both of these methods, use the Greeks for samples of the

4

input portfolio to estimate the Greeks of the full input portfolio. RSS requires several iterations of sample generation and evaluation to converge to a final result. This makes it more computationally demanding than the Kriging based techniques of (Gan, 2013; Gan and Lin, 2015) that require MC simulations results for only one sample. We discuss in our earlier paper (Hejazi et al., 2015) how the Kriging based techniques of (Gan, 2013; Gan and Lin, 2015) can be categorized under a general spatial interpolation framework. The spatial interpolation framework generates a sample of VA contracts from the space in which the VA contracts of the input portfolio are defined. The Greeks for the sample are evaluated using nested MC simulations. The results of MC simulations are then used by a spatial interpolation technique to generate an estimate for the Greeks of the input portfolio.

In (Hejazi et al., 2015), we provide numerical and theoretical results comparing the efficiency and accuracy of different conventional spatial interpolation techniques, i.e., Kriging, IDW and RBF. Our results demonstrate that, while the Kriging method provides better accuracy than either the IDW method or the RBF method, it is less efficient and has a lower resolution. By lower resolution, we mean that the Kriging method can provide the Greeks for only the input portfolio in an efficient manner, while both the IDW method and the RBF method approximate the Greeks efficiently for each VA contract in the input portfolio.

## 3. Neural Network Framework

As we discuss in our earlier paper (Hejazi et al., 2015), spatial interpolation techniques can provide efficient and accurate estimation of the Greeks for a large portfolio of VA products. Although IDW and RBF methods provide better efficiency and resolution than Kriging methods, they are less accurate than Kriging methods. Our experiments in (Hejazi et al., 2015) demonstrate the significance of the choice of distance function on the accuracy of IDW and RBF methods. A manual approach to find the best distance function that minimizes the estimation error of the IDW and the RBF methods for a given set of input data is not straightforward and requires investing a significant amount of time. The difficulty in finding a good distance function diminishes the effectiveness of the IDW and the RBF methods.

In order to automate our search for an effective distance function while maintaining the efficiency of the IDW and the RBF methods, we propose a machine learning approach. In our proposed approach, we use an extended

5

version of the Nadaraya-Watson kernel regression model (Nadaraya, 1964; Watson, 1964) to estimate the Greeks. Assuming $y(z_1), \cdots, y(z_n)$ are the observed values at known locations $z_1, \cdots, z_n$, the Nadaraya-Watson estimator approximates the value $y(z)$ at the location $z$ by

$$\hat{y}(z) = \sum_{i=1}^{n} \frac{K_h(z - z_i) \times y(z_i)}{\sum_{j=1}^{n} K_h(z - z_j)}$$

where $K_h$ is a kernel with a bandwidth of $h$. The Nadaraya-Watson estimator was first proposed for kernel regression applications and hence the choice of kernel function $K_h$ was a necessity. For our application of interest, we choose to use the following extended version of the Nadaraya-Watson estimator:

$$\hat{y}(z) = \sum_{i=1}^{n} \frac{G_{h_i}(z - z_i) \times y(z_i)}{\sum_{j=1}^{n} G_{h_j}(z - z_j)} \tag{1}$$

where $G$ is a nonlinear differentiable function and the subscript $h_i$, similar to the bandwidth $h$ of kernels, denotes the range of influence of each $y(z_i)$ on the estimated value. Unlike the Nadaraya-Watson model, the $h_i$s are not universal free parameters and are location dependent. Moreover, $h_i$ is a vector that determines the range of influence of each pointwise estimator in each direction of feature space of the input data. As we discuss below, our decision to calibrate the $h_i$ parameters using a neural network necessitated the properties of $G$.

In our application of interest, the $z_i, 1 \leq i \leq n$, in (1) define a set of VA contracts, called representative contracts, and $y(z_i), 1 \leq i \leq n$, are their corresponding Greek values. Hence, Equation (1) is similar to the equation for the IDW estimator. The $G_{h_i}(z - z_i)$ in (1) is comparable to the weight (inverse of the distance) for representative contract $z_i$ in the equation of IDW. Therefore, once we know the particular choices of the $h_i$s for the $G$ function for each of our $n$ representative VA contracts, we can compute the Greeks for a large portfolio of $N$ VA contracts in time proportional to $N \times n$, which preserves the efficiency of our framework. In order to find a good choice of the $G_{h_i}$ functions, we propose the use of a particular type of neural network called a feed-forward neural network. As we describe in more detail below, our choice of neural network allows us to find an effective choice of the $G_{h_i}$ functions by finding the optimum choices of the $h_i$ values that minimize our estimation error, and hence eliminate the need for a manual search of a good choice of distance function.
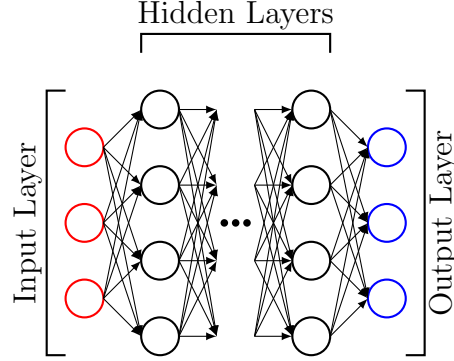
Figure 2: Diagram of a feed-forward neural network. Each circle represents a neuron.

Feed-forward networks are well-known for their general approximation properties which has given them the name of universal approximators. For example a one-layer feed-forward network with linear outputs is capable of approximating any continuous function on a compact domain (Hornik, 1991). For a thorough study of feed-forward networks, the interested reader is referred to (Bishop, 2006) and the references therein. For the sake of brevity, in the rest of this paper, we use the word neural network to refer to this particular class of feed-forward neural network unless explicitly said otherwise.

*3.1. The Neural Network*

A feed-forward neural network is a collection of interconnected processing units, called neurons, which are organized in different layers (Figure 2). The first and the last layers are respectively called the input layer and the output layer. Intermediate layers are called the hidden layers. Neurons of each layer take as input the outputs of the neurons in the previous layer. The neurons in the first layer serve only as inputs to the network. In other words, the neurons of the input layer produce what is known as the feature vector.

Assuming $x_1, \cdots, x_n$ are the inputs of neuron $j$ at hidden level $l$. First a linear combination of input variables is constructed at each neuron:

$$a_j^{(l)} = \sum_{i=1}^{n} w_{ij}^{(l)} x_i + b_j^{(l)}$$

where parameters $w_{ij}$ are referred to as weights and parameter $b_j$ is called the bias. The quantity $a_j^{(l)}$ is known as the activation of neuron $j$ at level
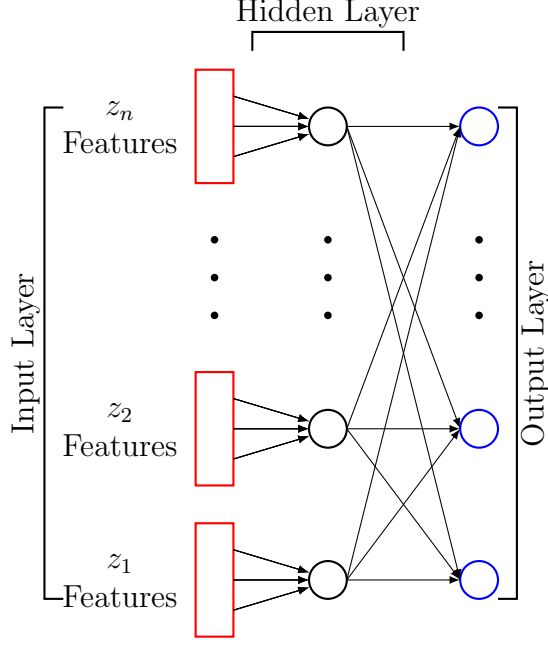
Figure 3: Diagram of the proposed neural network. Each circle represents a neuron. Each rectangle represent the set of neurons that contains input features corresponding to a representative contract.

$l$. The activation $a_j^{(l)}$ is then transformed using a differentiable, nonlinear function to give the output of neuron $j$ at level $l$.

In our framework, we propose to use a neural network with only one hidden layer (Figure 3). Each neuron in the input layer represents a value in the set $\{F^c, F^-, F^+\}$. Each $f$ in $F^c$ assumes the following form

$$f = \begin{cases} 0 & \text{if } x_c = x_{c_i} \\ 1 & \text{if } x_c \neq x_{c_i} \end{cases}$$

where $x_c$ represents the category of categorical attribute $c$ for input VA policy $z$, and $x_{c_i}$ represents the category of categorical attribute $c$ for representative VA policy $z_i$ in the sample. Each value $f$ in $F^-$ has the form $f = [t(\mathbf{x}_{n_i}) - t(\mathbf{x}_n)]^+/R_{t_h}$, and each value $f$ in $F^+$ has the form $f = [t(\mathbf{x}_n) - t(\mathbf{x}_{n_i})]^+/R_{t_h}$. In both of the aforementioned formulas, $\mathbf{x}_n$ is the vector containing the numeric attributes of input VA policy $z$, $\mathbf{x}_{n_i}$ is the vector containing the numeric attributes of representative VA policy $z_i$ in the sample, $t(\cdot)$ is a transformation (linear/nonlinear), determined by the expert

user, that assumes a value in an interval of length $R_t$ and $[\cdot]^+ = \max(\cdot, 0)$. In essence, our choice of input values allows different bandwidths ($h_i$ values in (1)) to be used for different attributes of VA policies and in different directions around a representative VA contract in the sample. Since we are interested in calibrating the $G$ functions of equation (1), the number of neurons in the output and hidden layer equals the number of representative contracts in the sample. The inputs of neuron $i$ in the hidden layer are those values of $f$ in the input layer that are related to the representative VA policy $i$. In other words, input values of neuron $i$ in the hidden layer determine the per attribute difference of input VA contract $z$ with the representative VA contract $z_i$ using the features $f \in \{F^c, F^-, F^+\}$. Each neuron of the hidden layer transforms its activation using an exponential function to form its output. The output of neuron $i$ in the output layer is the normalized version of the output for neuron $i$ in the hidden layer. Hence the outputs of the network, i.e., $o_i, i \in \{1, \cdots, n\}$, in machine learning terminology, correspond to a softmax of activations in the hidden layer. These outputs can be used to estimate the value of the Greek for input VA $z$ as $\hat{y}(z) = \sum_{i=1}^{n} o_i \times y(z_i)$, in which $y(z_i)$ is the value of the Greek for sample VA policy $z_i$. To summarize, our proposed neural network allows us to rewrite Equation (1) as

$$\hat{y}(z) = \sum_{i=1}^{n} \frac{\exp(\mathbf{w_i}^T \mathbf{f}(z, z_i) + b_i) \times y(z_i)}{\sum_{j=1}^{n} \exp(\mathbf{w_j}^T \mathbf{f}(z, z_j) + b_j)} \tag{2}$$

where vector $\mathbf{f}(z, z_i)$ represents the features in the input layer that are related to the representative VA policy $z_i$, and vector $\mathbf{w_i}$ contains the weights associated with each feature in $\mathbf{f}$ at neuron $i$ of the hidden layer. Each $\mathbf{w_i}$ in (2) can be considered as the pointwise inverse of the bandwidth value $h_i$ in (1).

### 3.2. Network Training Methodology

Equation (2) is a parametric formulation of our proposed estimator. We have to calibrate the weights and bias parameters to find an estimator with minimum estimation error. The calibration process, in neural network literature, is known as network training. In order to minimize the training time by reducing the number of VA policies for which the framework has to do MC estimations, we select a small set of VA policies which we call the training portfolio as the training data for the network. The objective of the calibration process is then to find a set of weights and bias parameters that

minimizes the Mean Squared Error (MSE) in the estimation of the Greeks of the training portfolio.

We choose the training portfolio to be different than the set of representative VA policies (i.e., observed points in the model (1)) to avoid data overfitting. Even with this choice of the training data, one cannot avoid the issue of overfitting. We discuss in Section 3.3 our solution to this problem.

Following the common practice in neural network literature, we use the following simple gradient descent scheme (Boyd and Vandenberghe, 2004) to iteratively update the weight and bias parameters.

$$[\mathbf{w}^{(t+1)}, \mathbf{b}^{(t+1)}] = [\mathbf{w}^{(t)}, \mathbf{b}^{(t)}] - \eta \nabla E(\mathbf{w}^{(t)}, \mathbf{b}^{(t)}) \tag{3}$$

The parameter $\eta > 0$ in (3) is known as the learning rate and $\mathbf{w}^{(t)}$ and $\mathbf{b}^{(t)}$ denote the vectors of the network's weights and biases, respectively, at iteration $t$. $E(\cdot)$ represents the error function that we are trying to minimize and $\nabla E$ is the gradient of $E$.

For a fair comparison with the traditional spatial interpolation techniques discussed in (Hejazi et al., 2015), training the network to minimize the following MSE in estimation of the Greeks for the training portfolio seems to be a reasonable approach.

$$E(\mathbf{w}, \mathbf{b}) = \frac{1}{2|B|} \sum_{k=1}^{|B|} ||\hat{y}(\bar{z}_k, \mathbf{w}, \mathbf{b}) - y(\bar{z}_k)||^2 \tag{4}$$

where $\bar{z}_k, 1 \leq k \leq |B|$, are the VA policies in the training portfolio.

Depending on the application of interest, the $y(\bar{z}_i)$ values can be too small (too big) resulting in too small (too big) gradient values for (4). Too small gradient values increase the training time to reach a local minimum, while too big gradient values cause big jumps in updates of (3) and hence numerical instability. Normalizing the values of $y(\bar{z}_i)$ in (4) and the choice of learning rate can help to ameliorate this problem.

Currently, in the field of machine learning, there does not exist a universal objective approach for choosing the values of the free parameters, such as the learning rate, that we describe in this section. Choosing appropriate values of almost all of these free parameters requires subjective judgement and is dependent on the data that is used and the application of interest. Although there exist many theoretical results (Boyd and Vandenberghe, 2004) that show that a particular choice of these parameters, e.g., learning rate,

can guarantee bounds on the convergence rate of the training method and these results are helpful in setting the theoretical framework for the training method, experimentation and subjective judgement must still be used to determine the actual values of many of these parameters. For example, for many problems, it is possible to prove that, if the the learning rate is sufficiently small, then the gradient descent method (3) will converge to a local minimum. Unfortunately, this result, or similar well-known results in the optimization or machine learning literature, do not say how to choose a "good" value for the learning rate that will ensure that the gradient descent method (3) yields near optimal values of the neural network parameters with an amount of computational work that is close to minimal. However, there is a well-established heuristic approach on how to choose the free parameters to meet this goal and/or to avoid problems such as overfitting (see, for example, (Murphy, 2012; Bishop, 2006) and references there in). Based on these guidelines, in Appendix A, we explain some simple heuristics that allow one easily to choose the free parameters described in this section.

Our formulation of error function (4) uses the whole training set to compute the error function and subsequently the gradient of the error function in each iteration. Training techniques that use the whole training set in each iteration are known as batch methods (Bishop, 2006). Because of the redundancy in the data as well as the computational complexity of evaluating gradients, batch gradient descent is a slow algorithm for training the network. Our experiments, further, corroborated the slowness of batch gradient descent in training our proposed network. To speed up the training, we used a particular version of what is known as the mini-batch training method (Murphy, 2012). In our training method, in each iteration, we select a small number ($\leq 20$) of training VA policies at random and train the network using the gradient of the error function for this batch. Hence, the error function in our mini-batch training method has the form

$$E(\mathbf{w^{(t)}}, \mathbf{b^{(t)}}) = \frac{1}{2|B^{(t)}|} \sum_{k \in B^{(t)}} ||\hat{y}(\bar{z}_k, \mathbf{w^{(t)}}, \mathbf{b^{(t)}}) - y(\bar{z}_k)||^2 \qquad (5)$$

where $B^{(t)}$ is the set of indices for selected VA policies at iteration $t$.

Gradient descent methods, at each iteration, produce a higher rate of reduction in the directions of high-curvature than in the directions of lower-curvature. Big rate reductions in directions of high-curvature cause zig-zag movements around a path that converges to the local minimum and hence

11

decrease the convergence rate (Murphy, 2012). However, a slower rate of reduction in directions of low-curvature allows for a persistent movement along the path of convergence to the local minimum. We can exploit this property by changing the weight update policy of gradient descent to use a velocity vector that increases in value in the direction of persistent reduction in the objective error function across iterations. This techniques is known as the momentum method (Polya, 1964). In our training method, we use Nestrov's Accelerated Gradient (NAG) method (Nesterov, 1983) which can be considered as a variant of the classical momentum method (Polya, 1964). In particular, we use a version of the NAG method described in (Sutskever et al., 2013) in which the NAG updates can be written as

$$v_{t+1} = \mu_t v_t - \epsilon \nabla E([\mathbf{w}^{(t)}, \mathbf{b}^{(t)}] + \mu_t v_t)$$
$$[\mathbf{w}^{(t+1)}, \mathbf{b}^{(t+1)}] = [\mathbf{w}^{(t)}, \mathbf{b}^{(t)}] + v_{t+1}$$

where $v_t$ is the velocity vector, $\mu_t \in [0, 1]$ is known as the momentum coefficient and $\epsilon$ is the learning rate. In this scheme, the momentum coefficient is an adaptive parameter defined by

$$\mu_t = \min(1 - 2^{-1-\log_2(\lfloor \frac{t}{50} \rfloor + 1)}, \mu_{\max}) \tag{6}$$

where $\mu_{\max} \in [0, 1]$ is a user defined constant. For general smooth convex functions and a deterministic gradient, NAG achieves a global convergence rate of $O(\frac{1}{T^2})$ [1] versus the $O(\frac{1}{T})$ convergence rate for gradient descent in which $T$ denotes the number of iterations (Sutskever et al., 2013). In this context, the rate of convergence is defined as the rate at which the error, $|f(x_T) - f(x^*)|$, goes to zero, where $f$ is a smooth convex function, $x^*$ is the optimum value (value of interest) and $x_T$ is the estimation of $x^*$ after iteration $T$.

### 3.3. Stopping Condition

Figure 4 represents a graph of the MSE for a set of training VA policies as a function of the training iteration number for one run of our training algorithm. The graph, except at a few points, is a decreasing function of the

---

[1]f(x) = O(g(x)) means that there exist positive numbers $c$ and $M$ such that $\forall x > M : f(x) < cg(x)$
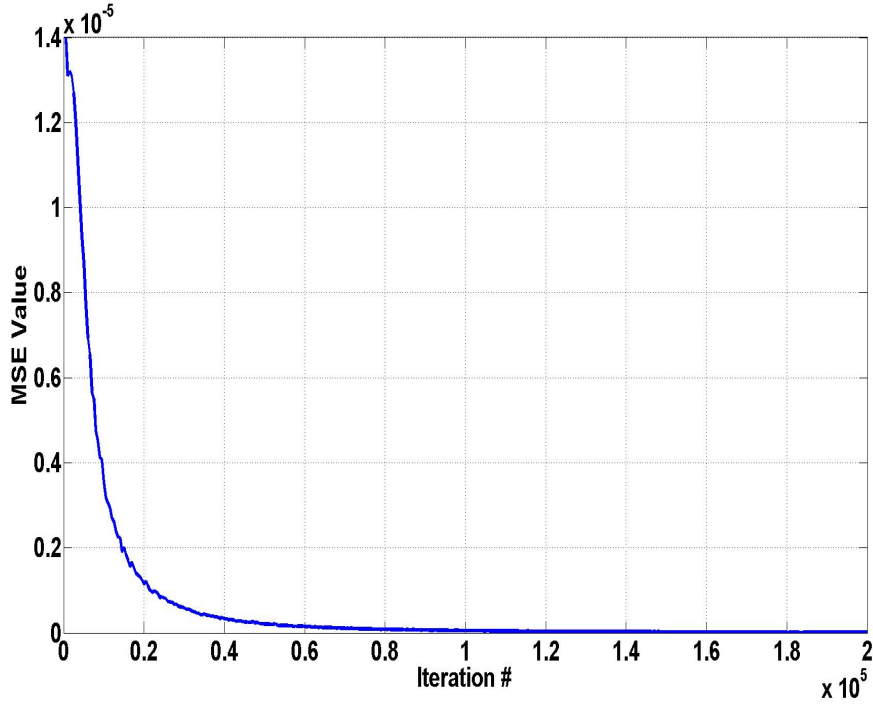
Figure 4: MSE of VA policies in the batch as a function of the iteration number.

iteration number which means that, as the iteration proceeds, the network is learning and steadily improving the bandwidth parameters for the model (2). After the first few thousand iterations, the graph of Figure 4 kneels and the rate of decrease in MSE drops dramatically. Such significant drops in the rate of MSE reduction is a sign that the network parameters are close to their respective optimum values. If we train the network for a longer time, we expect the MSE to continue to decrease slowly. However, the amount of improvement in the accuracy of the network might not be worth the time that we spend in further training the network. Hence, it might be best to stop the training.

If we select VA policies for the training portfolio very close to the representative VA policies, training the network for a long time can cause data overfitting. Because a perfect solution for (2), in this case, is achieved when the bandwidth values tend to zero or equivalently the weight parameters become very large. However, such a network approximates the Greeks of VA policies that are not close to the representative VA policies by zero. To avoid

13

over-training the network in such scenarios, we follow the common practice in the machine learning literature and track the MSE for a set of VA policies which we call the validation portfolio (Murphy, 2012). The validation portfolio is a small set of VA policies that are selected uniformly at random from the VA policies in the input portfolio. The MSE of the validation set should decrease at first as the network learns optimal parameters for the model (2). After reaching a minimum value, the MSE of the validation portfolio often increases as the network starts to overfit the model (2) (Figure 5). In our training method, we propose to evaluate the MSE of the validation portfolio every $I^{th}$ iteration of training, to avoid significantly slowing down the training process. We also propose to use a window of length $W$ of the recorded MSE values for the validation set to determine if the MSE of the validation set has increased in the past $W - 1$ recorded values after attaining a minimum. If we find such a trend, we stop the training to avoid overfitting. $I$ and $W$ are user defined (free) parameters and are application dependent.

As shown in the graph of Figure 5, the actual graph of the MSE for the validation portfolio as a function of iteration number might be volatile. However, a general u-shaped trend still exists in the data, which illustrates an increase in the value of the MSE after the MSE has reached a minimum. In order to find the trend graph, we use a simple moving average with a window size of $\bar{W}$ to smooth the data. We then fit, in the MSE sense, a polynomial of degree $d$ to the smoothed data. We examine the resulting trend graph with windows of length $W$ to determine the phenomenon of the MSE increase after attaining a local minimum. The parameters $\bar{W}$ and $d$ are free parameters and are dependent on the application of interest.

So far, we have discussed two events, which we call stopping events, that can be used as indicators to stop the training. In both events, the network parameters are close to optimal network parameter values. At this point, each additional iteration of the training algorithm moves these parameters in a neighborhood of the optimal values and might make the network parameters closer to the optimal values or farther from the optimal values. Intuitively, the best time to stop the training is when the network parameters are very close to the optimal values and further training does not significantly improve them. In our training algorithm, we propose to use the relative error in an estimation of the mean of the Greeks of the validation portfolio as our stopping criteria. Let $\bar{G_{NN}}$ and $\bar{G_{MC}}$ denote the mean of the estimated Greeks for the validation portfolio computed by our proposed neural network approach and by MC simulations respectively. The relative error in estimation of the
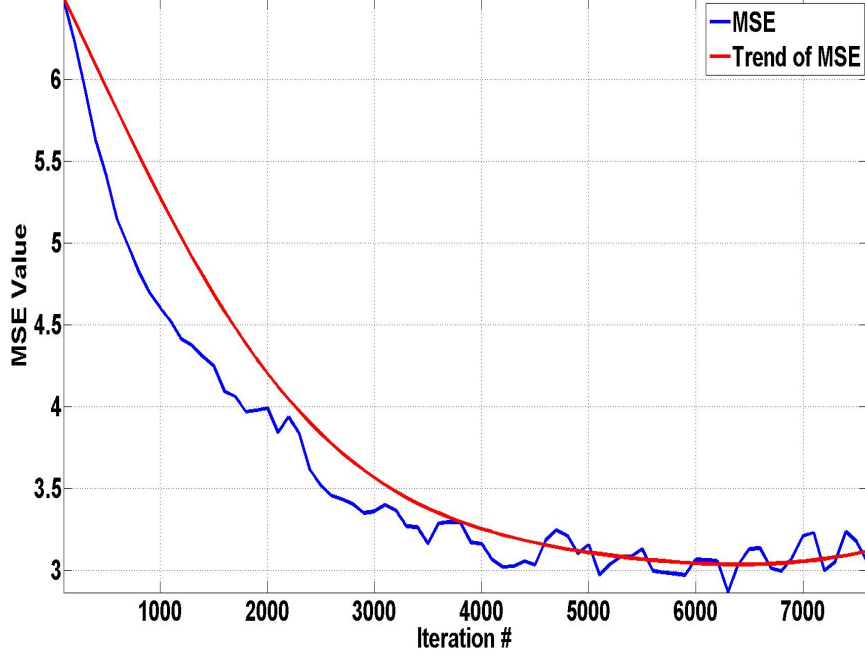
Figure 5: The MSE of the validation set and the trend in the MSE as a function of the iteration number for a run of the training algorithm. The trend is found using a moving average with a window size of 10 and then fitting a polynomial of degree 6 to the smoothed data.

mean of the Greeks for the validation portfolio is then

$$\text{Err} = \frac{|\bar{G_{NN}} - \bar{G_{MC}}|}{|\bar{G_{MC}}|} \tag{7}$$

If the relative error (7) is smaller than a user defined threshold $\delta$, we stop the training. The idea behind our choice of stopping criteria is that a good validation portfolio should be a good representative of the input portfolio. Hence, a network that has, on average, an acceptable accuracy in an estimation of the Greeks for the validation portfolio should, intuitively, have an acceptable accuracy in an estimation of the Greeks for the input portfolio as well. In some cases, finding stopping events and satisfying the stopping criteria may require the training algorithm to go through too many iterations, which can significantly increase the training time of the network and

15

consequently decrease the efficiency of the method. We propose to stop the training algorithm once the network has gone through a user defined maximum number of iterations to limit the training time in such scenarios.

*3.4. Sampling*

As we discuss in our earlier paper (Hejazi et al., 2015), the choice of an appropriate sampling method is a key factor in obtaining an effective method within the proposed spatial interpolation framework. Although we do not address the issue of selecting an effective sampling method in this paper, in this section, we describe ways in which the choice of our representative VA contracts can affect the performance of our proposed method.

Consider a realization of our proposed network with three representative contracts $x_1, x_2^{(1)}$ and $x_3$ with similar guarantee types. The VA contracts $x_1$ and $x_2^{(1)}$ are similar in every attribute except for the numeric attribute $a_n$ and they differ with VA contract $x_3$ in every attribute. Now, consider another realization of our proposed network in which we replace $x_2^{(1)}$ in the aforementioned realization with $x_2^{(2)}$. We choose $x_2^{(2)}$ such that it has similar categorical attributes as $x_2^{(1)}$; however, its numeric attributes assume the average of the corresponding numeric values for $x_1$ and $x_3$. Assume we train both networks for a similar number of iterations $I$. The gradient values of the error function depend only on the network architecture and the choice of input values. Since the input values for the corresponding hidden layer neurons for $x_1$ and $x_2^{(1)}$ in the former network are almost equal we expect the corresponding weight vectors $\mathbf{w_1^{(1)}}$ and $\mathbf{w_2^{(1)}}$ for these neurons to be approximately equal as well. However, because of the dissimilarity of the $x_1$ and $x_2^{(2)}$ contracts in the second network, we expect the input values and hence the corresponding weights $\mathbf{w_1^{(2)}}$ and $\mathbf{w_2^{(2)}}$ of the hidden layer neurons corresponding to these contracts to be quite different. Consequently, the latter network can provide a better differentiation between the $x_1$ and $x_2^{(2)}$ contracts while the former network requires more training time to provide the same level of accuracy in differentiating $x_1$ and $x_2^{(1)}$. Moreover, in approximating the Greeks for VA contracts other than $x_1, x_2^{(1)}, x_2^{(2)}$ and $x_3$, the former network, because of the similarity in weights $\mathbf{w_1^{(1)}}$ and $\mathbf{w_2^{(1)}}$, puts more emphasis on the corresponding Greeks of the contracts $x_1$ and $x_2^{(1)}$. Moreover, the latter network, because of the choice of $x_2^{(2)}$, can provide better accuracy for VA contracts that are quite different than both $x_1$ and $x_3$. Therefore, as demonstrated by this example, a bad sample can hurt the efficiency of the proposed

| Attribute | Value |
|---|---|
| Guarantee Type | {GMDB, GMDB + GMWB} |
| Gender | {Male, Female} |
| Age | $\{20, 21, \ldots, 60\}$ |
| Account Value | $[1e4, 5e5]$ |
| Guarantee Value | $[0.5e4, 6e5]$ |
| Withdrawal Rate | $\{0.04, 0.05, 0.06, 0.07, 0.08\}$ |
| Maturity | $\{10, 11, \ldots, 25\}$ |

Table 1: GMDB and GMWB attributes and their respective ranges of values.

method by requiring more training time. Moreover, a bad sample can hurt the accuracy of the proposed network in estimation of the Greeks of VA contracts that assume attribute values that are different than the representative contracts, in particular those VA contracts that are quite distant from any representative contract.

## 4. Numerical Experiments

In this section, we provide numerical results illustrating the performance of the proposed neural network framework in comparison with the traditional spatial interpolation schemes (i.e., Kriging, IDW, and RBF) discussed in (Hejazi et al., 2015). The input portfolio in all experiments is a synthetic portfolio of 100,000 VA contracts with attribute values that are chosen uniformly at random from the space described in Table 1. Similar to (Hejazi et al., 2015), we allow guarantee values to be different than the account values. The guaranteed death benefit of contracts with a GMWB rider is set to be equal to their guaranteed withdrawal benefit. The account values of the contracts follow a simple log-normal distribution model (Hull, 2006) with a risk free rate of return of $\mu = 3\%$, and volatility of $\sigma = 20\%$.

In our experiments, we use the framework described in (Gan and Lin, 2015) to value each VA contract. In each MC simulation, even in the calibration stage of the interpolation schemes to value representative contracts, we use 10,000 scenarios. Fewer scenarios results in a noticeable difference, as big as 5%, between the computed delta value from successive runs. In our experiments, we use mortality rates of the 1996 I AM mortality tables provided by the Society of Actuaries.

|  | Experiment 1 |
|---|---|
| Guarantee Type | {GMDB, GMDB + GMWB} |
| Gender | {Male, Female} |
| Age | $\{20, 30, 40, 50, 60\}$ |
| Account Value | $\{1e4, 1e5, 2e5, 3e5, 4e5, 5e5\}$ |
| Guarantee Value | $\{0.5e4, 1e5, 2e5, 3e5, 4e5, 5e5, 6e5\}$ |
| Withdrawal Rate | $\{0.04, 0.08\}$ |
| Maturity | $\{10, 15, 20, 25\}$ |

Table 2: Attribute values from which representative contracts are generated for experiments.

We implement the framework in Java and run it on machines with dual quad-core Intel X5355 CPUs. We do not use the multiprocessing capability of our machine in these experiments; however, in our future work, we will demonstrate that even the serial implementation of our proposed framework can provide better efficiency than parallel implementation of MC simulations.

*4.1. Representative Contracts*

As we discuss above in Section 3, we do not address the issue of an effective sampling method in this paper. Hence, in all of the experiments in this section, we use a simple uniform sampling method similar to that in (Hejazi et al., 2015). In each set of experiments, we select 300 representative contracts from the set of all VA contracts constructed from all combinations of points defined in Table 2. In a set of experiments, we select a set of representative contracts at the beginning of the experiment, and use the same set for various spatial interpolation methods that we examine in that experiment. This allows for a fair comparison between all methods.

*4.2. Training/Validation Portfolio*

Unlike traditional spatial interpolation schemes, we need to introduce two more portfolios to properly train our neural network. In each set of experiments, we select 250 VA contracts uniformly at random from the input portfolio as our validation portfolio.

For the training portfolio, we select 200 contracts uniformly at random from the set of VA contracts of all combinations of attributes specified in Table 3. The attributes of Table 3 are intentionally different from the attributes of Table 2 to avoid unnecessary overfitting of the data.

|  | Experiment 1 |
|---|---|
| Guarantee Type | {GMDB, GMDB + GMWB} |
| Gender | {Male, Female} |
| Age | $\{23, 27, 33, 37, 43, 47, 53, 57\}$ |
| Account Value | $\{0.2e5, 1.5e5, 2.5e5, 3.5e5, 4.5e5\}$ |
| Guarantee Value | $\{0.5e5, 1.5e5, 2.5e5, 3.5e5, 4.5e5, 5.5e5\}$ |
| Withdrawal Rate | $\{0.05, 0.06, 0.07\}$ |
| Maturity | $\{12, 13, 17, 18, 22, 23\}$ |

Table 3: Attribute values from which training contracts are generated for experiments.

### 4.3. Parameters Of The Neural Network

In our numerical experiments, we use the following set of parameters to construct and train our network. We choose a learning rate of 1. We set $\mu_{\max}$ in (6) to 0.99. We use a batch size of 20 in our training. We fix the seed of the pseudo-random number generator that we use to select batches of the training data so that we can reproduce our network for a given set of representative contracts, training portfolio, and validation portfolio. Moreover, we initialize our weight and bias parameters to zero.

The categorical features in $F^c$ are rider type and gender of the policy-holder. The following numeric features make up $F^+$.

$$f(z, z_i) = \frac{[t(x) - t(x_i)]^+}{R_t} \tag{8}$$

$$t \in \{\text{maturity, age, AV, GD/AV, GW/AV, withdrawal rate}\}$$

where $AV$ is the account value, $GD$ is the guaranteed death benefit, $GW$ is the guaranteed withdrawal benefit, $R_t$ is the range of values that $t$ can assume, $x$ is the vector of numeric attributes for input VA contract $z$, and $x_i$ is the vector of numeric attributes for representative contract $z_i$. The features of $F^-$ are defined in a similar fashion by swapping $x$ and $x_i$ on the right side of Equation (8).

We record MSE every 50 iterations. We compute a moving average with a window of size 10 to smooth the MSE values. Moreover, we fit, in a least squares sense, a polynomial of degree 6 to the smoothed MSE values and use a window of length 4 to find the trend in the resulting MSE graph. In addition, we choose a $\delta$ of 0.005 as our threshold for the relative error in estimation of the Greeks for the validation portfolio.

### 4.4. Performance

In these experiments, we compare the performance (i.e., accuracy, efficiency, and granularity) of our proposed neural network scheme, referred to as $NN$ in the results tables, with that of the traditional spatial interpolation schemes. From the set of interpolation techniques discussed in (Hejazi et al., 2015), we choose only the following interpolation methods with a corresponding distance function which exhibited the most promising results in (Hejazi et al., 2015).

- Kriging with Spherical and Exponential variogram models,

- IDW with power parameters $P$ of 1 and 100,

- Gaussian RBF with free parameter $\epsilon$ of 1.

The distance function for the Kriging and RBF methods is

$$D(\mathbf{x}, \mathbf{y}, \gamma) = \sqrt{\sum_{h \in N} \left( \frac{x_h - y_h}{\max_h - \min_h} \right)^2 + \gamma \sum_{h \in C} \delta(x_h, y_h)}$$

where $N = \{$AV, GD, GW, maturity, age, withdrawal rate$\}$ is the set of numerical values and $C = \{$gender, rider$\}$ is the set of categorical values, and $\gamma = 1$.

For the IDW methods we choose the following distance function that provided the most promising results in (Hejazi et al., 2015).

$$D(\mathbf{x}, \mathbf{y}, \gamma) = \sqrt{f(x_{\text{age}}, y_{\text{age}}) g_{\text{age}}(\mathbf{x}, \mathbf{y}) + \sum_{h \in N} g_{\text{h}}(\mathbf{x}, \mathbf{y}) + \gamma \sum_{h \in C} \delta(x_h, y_h)}$$

$$f(x_{\text{age}}, y_{\text{age}}) = \exp \left( \frac{x_{\text{age}} + y_{\text{age}}}{2} - M \right)$$

$$g_h(\mathbf{x}, \mathbf{y}) = (\exp(-r_x) x_h - \exp(-r_y) y_h)^2$$

where $C = \{$gender, rider$\}$, $N = \{$maturity, withdrawal rate$\}$, $r = \frac{AV}{GD}$ and $M$ is the maximum age in the portfolio.

Because we randomly select our representative contracts according to the method described in Section 4.1, we compare the performance of the interpolation schemes using 6 different realizations of the representative contracts, $Si, 1 \leq i \leq 6$. For our proposed neural network approach, we use the same

| Method | Relative Error (%) | | | | | |
|---|---|---|---|---|---|---|
| | S1 | S2 | S3 | S4 | S5 | S6 |
| Kriging (Sph) | −0.60 | 0.55 | 7.62 | 2.86 | 2.58 | 3.59 |
| Kriging (Exp) | −0.29 | 1.73 | 8.09 | 4.77 | 3.46 | 4.38 |
| IDW (p = 1) | −21.43 | −14.48 | −21.76 | −7.22 | −12.47 | −11.77 |
| IDW (p = 100) | −11.74 | −7.81 | −4.36 | −0.07 | −2.72 | −2.45 |
| RBF (Gau, $\epsilon = 1$) | −0.76 | −5.21 | −10.45 | −7.83 | 2.47 | 4.11 |
| NN | −1.16 | 0.84 | 1.56 | 0.85 | 1.66 | −1.46 |

Table 4: Relative error in estimation of the portfolio's delta value by each method.

training portfolio and validation portfolio in all of these 6 experiments. We study the effect of the training portfolio and the validation portfolio in a different experiment.

Table 4 displays the accuracy of each scheme in estimation of the delta value for the input portfolio. The accuracy of different methods is recorded as the relative error

$$\text{Err}_m = \frac{\Delta_m - \Delta_{MC}}{|\Delta_{MC}|} \qquad (9)$$

where $\Delta_{MC}$ is the estimated delta value of the input portfolio computed by MC simulations and $\Delta_m$ is the estimate delta value of the input portfolio computed by method $m$. The results of Table 4 show the superior performance of our proposed neural network (NN) framework in terms of accuracy. Except in a few cases, the accuracy of our proposed NN framework is better than all of the other interpolation schemes. The Spherical Kriging has the best performance amongst the traditional interpolation schemes. Comparing the accuracy results of our proposed neural network scheme with that of Spherical Kriging shows that the relative error of the proposed scheme has lower standard deviation and hence is more reliable.

In Table 5, the average training and estimation time of each method is presented for two scenarios: (1) the method is used to estimate only the delta value of the entire portfolio and (2) the method is used to estimate the delta value of each policy in the input portfolio. Because of the complex calculations required to train the proposed NN method, the running time of the proposed NN method is longer than that of the traditional interpolation scheme. However, it still outperforms the MC simulations (speed up of > ×15).

| Method | Portfolio | Per Policy |
|---|---|---|
| MC | 10617 | 10617 |
| Kriging (Spherical) | 41 | $\gg 10617$ |
| Kriging (Exponential) | 41 | $\gg 10617$ |
| IDW (P = 1) | 29 | 29 |
| IDW (P = 100) | 28 | 28 |
| RBF (Gaussian, $\epsilon = 1$) | 41 | 41 |
| NN | 539 | 539 |

Table 5: Simulation time of each method to estimate the delta value. All times are in seconds.

In this experiment, assuming no prior knowledge of the market, we used the value of zero as our initial value for weight/bias parameters which is far from the optimal value and causes the performance of the proposed NN method to suffer from a long training time. In practice, insurance companies estimate the Greeks of their portfolios on frequent intraday basis to do dynamic hedging. Assuming a small change in the market condition, one does not expect the Greek values of the VA policies to change significantly. Hence, intuitively, the change in the optimal values of weight/bias parameters of the network under the previous and the current market conditions should be small. In our future paper, in the context of estimating the probability distribution of the one year loss, we will demonstrate how we exploit this fact to reduce the training time of the network from an average of 4000 iterations to less than 200 iterations and hence reduce the training time significantly. In particular, assuming a neural network that has been calibrated to the previous market conditions, we construct a new network that uses the values of the weight/bias parameters of the previous network as the initial values for the weight/bias parameters in the training stage.

A comparison of the running time in the two columns of Table 5 shows that the proposed NN method, similar to IDW and RBF, can be used to efficiently provide a granular view of the delta values in the input portfolio. Figure 6 shows a granular view of the estimated delta values by our proposed NN scheme for the validation portfolio. As shown in the figure, the NN estimated delta values closely follow their corresponding MC estimated values (plotted data values are very close to the line $y = x$). In particular, the majority of data points are within a distance of 0.1 of the $y = x$ line (the red line). Moreover, the data points are distributed almost uniformly around
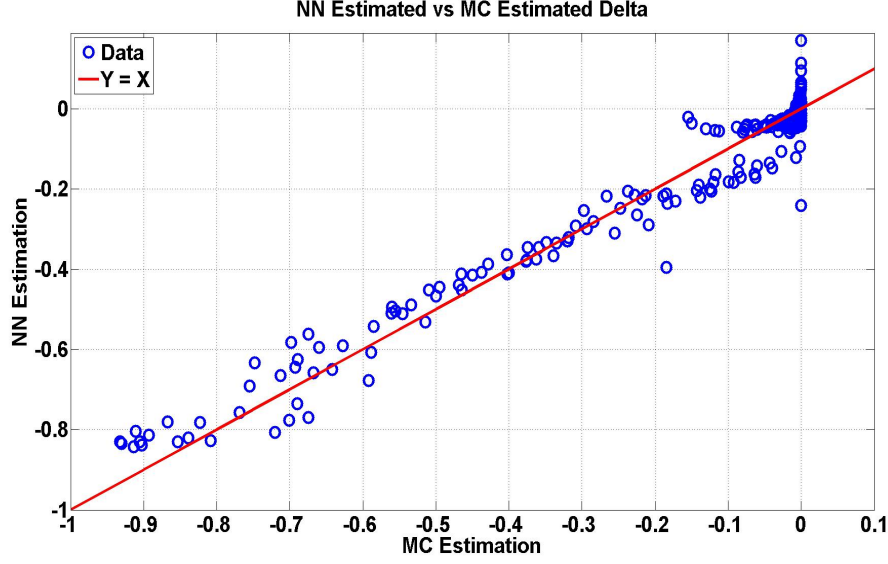
Figure 6: Estimated delta values of the validation portfolio by MC simulations and the neural network.

the red line. In other words, the amount of over estimations by the neural network is close to the amount of under estimations by the neural network. Therefore, the estimation errors, in aggregate, cancel each other out, resulting in a smaller portfolio error than might be expected from looking at the maximum absolute error alone in Figure 6.

The graph also shows a cluster of points around the origin. In fact, the majority of the points are very close to the origin with only a few points deviating relatively far in each direction. These few points do not significantly affect the accuracy, especially when the estimations are accurate for big delta values.

*4.5. Sensitivity to Training/Validation Portfolio*

The training of our proposed NN method requires the selection of three VA portfolios. In the experiments of Section 4.4, we fix the selection of two of these portfolios (i.e., training portfolio and validation portfolio) while we measured the performance of our proposed method by changing the set of representative contracts. In the experiments of this section, we investigate the sensitivity of the accuracy and efficiency of our proposed method to the choice of training and validation portfolio. We conduct two sets of experi-

| Variable Portfolio | Relative Error (%) | | Running Time | |
|---|---|---|---|---|
| | Mean | STD | Mean | STD |
| Training | 0.27 | 1.52 | 660 | 246 |
| Validation | −0.62 | 1.51 | 523 | 38 |

Table 6: Statistics on the running time sensitivity and accuracy sensitivity of the training network with different sets of training and validation portfolios. The recorded errors are relative errors as defined in (9). All times are in seconds.

ments in which we fix the choice of representative contracts and either the training portfolio or the validation portfolio, while training the network with different realizations of the remaining portfolio. In the first set of experiments, we fix the choice of the representative contracts and the validation portfolio. We train the network with 5 different choices of the training portfolio and estimate the delta value of the input portfolio in each experiment. In the second set of experiments, we fix the choice of the representative contracts and the training portfolio and train the network with 5 different realizations of the validation portfolio. We then use the trained network to estimate the delta value of the input portfolio in each experiment. We used the same set of representative contracts in both set of experiments.

The statistics for the running time (training and estimation) and accuracy of each set of experiments are presented in Table 6. The relatively big values of the standard deviations indicate that the accuracy of the estimation is sensitive to the choice of the training portfolio and the validation portfolio. Despite this sensitivity, the method remains accurate.

The choice of the training portfolio can significantly affect the running time of the neural network; however, the running time of the network is fairly insensitive to changes in the choice of validation portfolio. The validation portfolio in the training is mainly used as a guard against over fitting. It is a useful stopping criteria to fine tune the network once we are close to the local optimum. But the training portfolio controls the path that the training takes to arrive at a neighborhood close to the local optimum. A bad training portfolio can slow the training by introducing a large deviation from a consistent path towards the local optimum. Hence the choice of the training portfolio has a more significant effect than the choice of the validation portfolio on the running time.

| Portfolio Sizes | Relative Error (%) | | Running Time | |
|---|---|---|---|---|
| | Mean | STD | Mean | STD |
| $(300, 200, 250)$ | 0.38 | 1.35 | 539 | 120 |
| $(250, 200, 250)$ | $-0.73$ | 1.42 | 373 | 73 |
| $(200, 200, 250)$ | $-1.62$ | 1.52 | 310 | 85 |
| $(300, 200, 250)$ | 0.27 | 1.52 | 539 | 246 |
| $(300, 150, 250)$ | $-4.31$ | 7.66 | 708 | 254 |
| $(300, 100, 250)$ | 6.50 | 14.47 | 669 | 303 |
| $(300, 200, 250)$ | $-0.62$ | 1.51 | 523 | 38 |
| $(300, 200, 200)$ | 0.70 | 3.23 | 511 | 24 |
| $(300, 200, 150)$ | 2.31 | 3.67 | 582 | 188 |

Table 7: Statistics on running time sensitivity and accuracy sensitivity of training network with portfolios of various sizes. The recorded errors are relative errors as defined in (9). All times are in seconds.

### 4.6. Sensitivity to Sample Sizes

In the previous experiments, we examined the sensitivity of our proposed neural network framework to the selection of the training portfolio, the validation portfolio, and the set of representative contracts. In this section, we conduct experiments that assess the sensitivity of our proposed framework on the size of these portfolios. In each experiment, we fix two out of the three required portfolios while changing the size of the third portfolio. For each selected size of the latter portfolio, we train the network with 5 realizations of the portfolio and record the running time and accuracy of the method.

Table 7 contains the statistics on the recorded running time and the relative error for each set of selected portfolio sizes. Each row in the table begins with a tuple $(r, t, v)$ denoting the size of the set of representative contracts, the training portfolio, and the validation portfolio, respectively. In the scenarios corresponding to the first three rows, we changed the size of representative contracts. The second three rows show the results for the scenarios in which we changed the size of the training portfolio. Finally, in the scenarios corresponding to the third three rows, we changed the size of the validation portfolio.

The results of Table 7 show that decreasing the number of representative contracts increases the efficiency of the network. Furthermore, the amount of decrease in running time is proportional to the amount of decrease in the

number of representative contracts. This result is expected since the number of calculations in the network is proportional to the number of neurons in the hidden layer which is proportional to the number of representative contracts. Although the accuracy of the method deteriorates as we decrease the number of representative contracts, the accuracy of the worst network is still comparable to the best of the traditional spatial interpolation techniques (see Table 4). Hence, if required, we can sacrifice some accuracy for better efficiency.

According to the statistics in the second set of three rows of Table 7, decreasing the size of the training portfolio can significantly affect the accuracy of the method. Decreasing the number of training VA contracts results in a poorer coverage of the space in which the network is trained. In the space where the training VA contracts are sparse, the parameters of the representative VA contracts are not calibrated well, resulting in poor accuracy of estimation. Although the mean of the simulation time does not consistently decrease with the decrease in the size of the training portfolio, the standard deviation of the simulation time increases significantly. The increase in the standard deviation of the network's simulation time is a further proof that the network is struggling to calibrate its parameters for the smaller training portfolios.

The results in the last three rows of Table 7 suggest that decreasing the size of validation portfolio decreases the accuracy of the proposed framework. The deterioration in the performance of the network is more apparent from the amount of increase in the standard deviation of the relative error values. As one decreases the size of the validation portfolio, the VAs in the validation portfolio provide a poorer representation of the input portfolio. Although the change in the accuracy of the method is significant, the running time of the method is less affected by the size of the validation portfolio, except for the validation portfolio of the smallest size, where one can see a big increase in the standard deviation of the running time.

As we mentioned earlier in Section 4.5, the validation portfolio only affects the last stage of the training where the network parameters are close to their local optimal values. When the size of the validation portfolio is too small, various realizations of the validation portfolio may not adequately fill the space resulting in portfolio delta values that differ significantly from one realization to another. Hence, the overlap between the $\delta$ neighborhood of the portfolio delta values for various validation portfolios and the local neighborhood of the optimal network parameter values may vary in place and size

26

significantly. The network stops the training as soon as it finds a set of network parameters that are within the aforementioned common neighborhood. Therefore, the training time of the network can vary significantly based on the size and the place of the common neighborhood. As the size of the common neighborhood increases, the network spends less time searching for a set of network parameters that are within the common neighborhood. Because the training time is a significant part of the running time of the proposed neural network scheme, the standard deviation of the running time increases as the result of the increase in the standard deviation of the training time.

## 5. Concluding Remarks

In recent years, a spatial interpolation framework has been proposed to improve the efficiency of valuing large portfolios of complex insurance products, such as VA contracts via nested MC simulations (Gan, 2013; Gan and Lin, 2015; Hejazi et al., 2015). In the proposed framework, a small set of representative VA contracts is selected and valued via MC simulations. The values of the representative contracts are then used in a spatial interpolation method that finds the value of the contracts in the input portfolio as a linear combination of the values of the representative contracts.

Our study of traditional spatial interpolation techniques (i.e., Kriging, IDW, RBF) (Hejazi et al., 2015) highlights the strong dependence of the accuracy of the framework on the choice of distance function used in the estimations. Moreover, none of the traditional spatial interpolation techniques can provide us with all of accuracy, efficiency, and granularity, as defined in (Hejazi et al., 2015).

In this paper, we propose a neural network implementation of the spatial interpolation technique that learns an effective choice of the distance function and provides accuracy, efficiency, and granularity. We study the performance of the proposed approach on a synthetic portfolio of VA contracts with GMDB and GMWB riders. Our results in Section 4 illustrate the superior accuracy of our proposed neural network approach in estimation of the delta value for the input portfolio compared to the traditional spatial interpolation techniques.

Although the proposed NN framework, compared with traditional spatial interpolation techniques, requires longer training time, it can interpolate the delta values of an input portfolio of size $N$ in a time proportional to $n \times N$ ($n$ is the number of samples), which is essentially the same as the time required

27

by the most efficient traditional spatial interpolation techniques IDW and RBF. Moreover, the proposed NN approach provides an efficient solution to the issue of choosing a distance function.

Training of the network requires us to introduce two additional sets of sample VA contracts, i.e., the training portfolio and the validation portfolio, compared to the traditional frameworks (Hejazi et al., 2015). Our experiments in Section 4 show that, if each of the aforementioned sample sets is sufficiently large, a random selection of these sets from a predefined set of VA contracts that uniformly covers the space of the input portfolio does not significantly affect the accuracy and efficiency of the method. However the size of each of these sample sets can significantly affect the performance of our proposed neural network approach.

Although this paper studies an important application of the proposed neural network framework, in the future, we will extend the approach to compute other key risk metrics. In particular, we will demonstrate the efficiency and accuracy of this framework in estimating the probability distribution of the portfolio loss, which is key to calculate the Solvency Capital Requirement.

## 6. Acknowledgements

## Appendix A. How To Choose The Training Parameters

The training method that we discuss in Section 3 is dependent on the choice of numerous free parameters such as the learning rate and $\mu_{\max}$. In this appendix, we discuss heuristic ways to choose a value for each of these free parameters and justify each choice.

In order to determine a good choice of the learning rate and the batch size, we need to train the network for some number of iterations, say 3000, and study the error associated with the training portfolio as a function of the number of iterations. If the graph has a general decreasing trend and it does not have many big jumps between consecutive iterations, then we say that the choice of the learning rate/batch size is stable. Otherwise, we call the choice of the learning rate/batch size unstable.

From (3), we see that the choice of the learning rate parameter affects the amount of change in the weight and bias parameters per iteration. As we
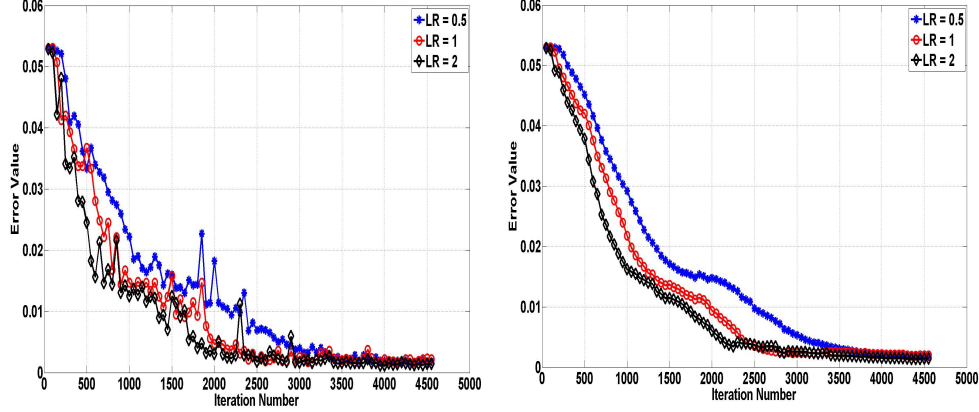
Figure A.7: The MSE error graph (left) and the moving average smoothed MSE error graph (right) of the training portfolio as a function of iteration number and learning rate.

discuss in Section 3.2, too small of a change increases the training time while too big of a change causes numerical instability. From Figure A.7, we see that, as we increase the value of the learning rate, the graph of the error values moves downwards which means that the training has sped up. However, for a learning rate equal to 2, we see many big jumps in the graph which suggests numerical instability. The numerical instability is more obvious from the moving average smoothed curve of error values. More specifically, starting from iteration 2000, the smoothed MSE error graph for a learning rate of 2 has big jumps which are signs of numerical instability. Note that the smoothed MSE error graphs for learning rates 0.5 and 1 are much smoother.

Although the MSE error graphs for learning rates 0.5 and 1 are stable, these graphs still contain big jumps, which are the result of using mini-batch training. As we discuss earlier, at each iteration, the mini-batch training method updates the weights in the direction of the gradient for the error function (5). As the definition suggests, the error (5) is dependent on the choice of the VA contracts in that particular mini-batch. Therefore, the direction of the gradient for this function may not align with the gradient of (4) which is defined over the complete batch (i.e., the training portfolio) and hence updating the weights along the direction of the gradient of (5) can move the weights away from their local minimum which contributes to the jumps that we see in the MSE error graph. Too many such misalignments can cause big jumps in the MSE error graph. Introducing momentum can to

some extent ameliorate this phenomenon but it cannot completely avoid it (Murphy, 2012; Sutskever et al., 2013). Furthermore, as we discuss in detail below, the size of the mini-batch that we choose affects the severity of these jumps. Hence, one should expect some jumps in the MSE error graph which determines the MSE error for estimation of the key risk metric of interest for all the VAs in the training portfolio. However, if big jumps happen too often, they may cause the weights to oscillate around the local minimum of the MSE error function or, even worse, they may force the weights to move away from the local minimum. Choosing an appropriate size for the mini-batch (as described below) usually helps to ameliorate this potential deficiency.

To find a good choice of the learning rate, we can start from a value of 1 for the learning rate and determine if that choice is stable? If the choice of learning rate is stable, we double the value of the learning rate and repeat the process until we find a learning rate which is unstable. At this point, we stop and choose the last stable value of the learning rate as our final choice of the learning rate. If the learning rate equal to 1 is unstable, we decrease the value of learning rate to half of its current value and repeat this process until we find a stable learning rate.

The batch size controls the speed of training and the amount of error that we get in approximating the gradient of the MSE for the entire training set. Small batch sizes increase the speed of training; however, they also increase the amount of error in approximating the gradient of the MSE error. A good batch size should be small enough to increase the speed of training but not so small as to introduce a big approximation error. To find a good batch size value, we start with a small value, say 5, and determine if this choice of batch size is stable. If so, we stop and choose it as our final choice of the batch size. If the batch size is unstable, we double the batch size and repeat the process until we find a stable batch size.

Figure A.8 shows that small batch size values are associated with many big jumps and hence are unstable. As we increase the batch size value, the error graph becomes much more stable– fewer jumps and a more consistent decreasing trend.

Notice that, in the aforementioned processes for finding the appropriate value of the learning rate and batch size, doubling the values may seem too aggressive as the values may increase or decrease too quickly. To alleviate this problem, upon reaching a desired value, we can do a binary search between the final choice of parameter's value and the next best choice (the value of
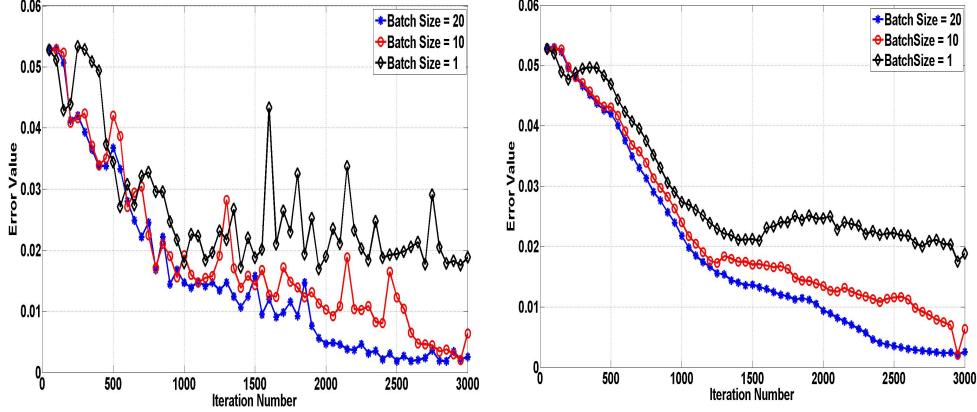
Figure A.8: The MSE error graph (left) and the moving average smoothed MSE error graph (right) of the training portfolio as a function of iteration number and batch-size.

parameter before the final doubling) of the parameter's value.

Nesterov, (Nesterov, 2003, 1983), advocates a constant momentum coefficient for strongly convex functions and advocates Equation (A.1) when the function is not strongly convex (Sutskever et al., 2013).

$$\mu_t = 1 - \frac{3}{t+5} \tag{A.1}$$

Equation (6), suggested in (Sutskever et al., 2013), blends a proposal similar to Equations (A.1) and a constant momentum coefficient. Equation (A.1) converges quickly to values very close to 1. In particular, for $t \geq 25$, $\mu_t \geq 0.9$. Hence, as suggested in (Sutskever et al., 2013), we should choose large values $(0.9, 0.99, 0.995, 0.999)$ of $\mu_{\max}$ to achieve better performance and that is what we suggest too.

In Section 3.3, we proposed a mechansim to detect stopping events and avoid over-training of the network. As part of this mechanism, we need to record the MSE of the validation set every $I^{th}$ iteration. Too small values of $I$ can slow down the training process while too big values of $I$ can result in losing the information regarding the trend that exists in the MSE graph. In order to find a good value of $I$ that neither slows down the training too much nor creates excessive information loss, we can use a multiplicative increase process similar to that described above for the batch size. We start with a small value of $I$, say 10, and train the network for some 4000 iterations and draw the graph of MSE values. We then double the $I$ value and graph
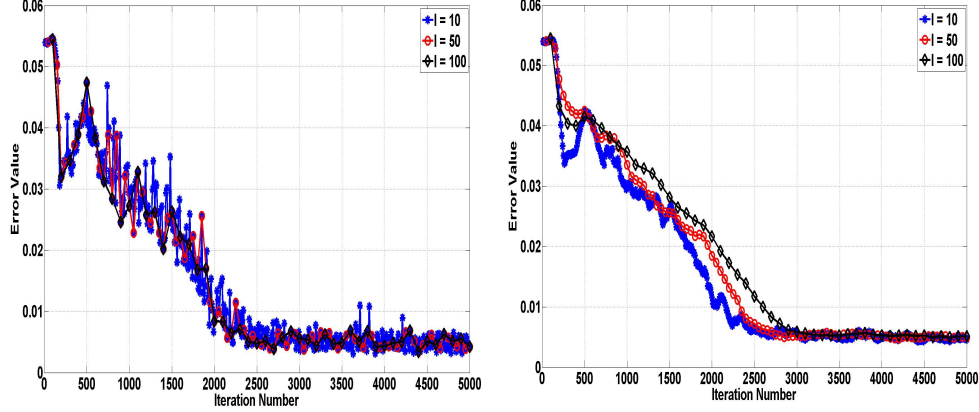
31

Figure A.9: The MSE error graph (left) and the moving average smoothed MSE error graph (right) of the validation portfolio as a function of iteration number and $I$ value.

the MSE for the new value of $I$. If the MSE graph for the new value of $I$ has a similar trend as the MSE graph for the previous value of $I$, we keep increasing the $I$ value and repeat the process. But, if the resulting graph has lost significant information regarding increasing/decreasing trends in the previous graph, then we stop and choose the previous value of $I$ as the appropriate choice of $I$. For example, in Figure A.9, the MSE graph corresponding to the value of 100 has fewer big valleys and big peaks than the MSE graph for the value of 50. Hence, we have lost a significant amount of information regarding trends in the graph. However, the MSE graph for the value of 10 has a roughly similar number of big valleys and big peaks compared with the MSE graph for the value of 50. Hence, the value of 50 is a much better choice for $I$ than either 100 or 10. The value of 50 allows for a faster training than the value of 10 and has more information regarding increasing/decreasing trends in the MSE error graph than the value of 100.

We use data smoothing and polynomial fitting to extract the major u-shape trend in the MSE graph and hence find stopping events. In order to find a good choice for the smoothing window, we start with a small value of the smoothing window and calculate the smoothed curve. If the small peaks and valleys of the orignial curve are supressed and big peaks and big valleys of the original curve are significantly damped, then we choose that value of the smoothing window as our final choice for the smoothing window. For example, in Figure A.10, the smoothed curve with a smoothing window of 5
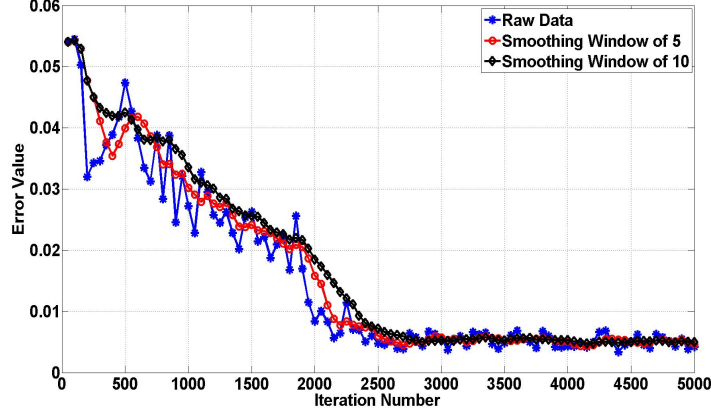
32

Figure A.10: The MSE error graph of the validation portfolio as a function of iteration number and smoothing window value.

still has a big valley around iteration number of 400. However the valley is dampened in the smoothed graph resulting from smoothing window of 10.

The primary goal of the polynomial fitting is to find the u-shaped trend in the graph so that we can detect the stopping event. The u-shaped trend therefore suggests that the polynomial should go to infinity as its argument goes to either plus or minus infinity. Therefore, the degree of the polynomial should be even. Since we are only interested in detecting a u-shaped trend, it is sufficient to use polynomials of low degree ($\leq 10$). High degree polynomials overfit the data and they can't detect a slowly increasing trend such as the one in Figure A.10 after iteration 2500. On the other hand, a simple polynomial of degree 2 does not always work well. A quadratic polynomial on a MSE graph similar to Figure A.10 falsely detects a u-shape trend in the big valley between iteration numbers 0 and 500. However a polynomial of degree 4 or higher will not make such a detection. Because we smooth the data before we fit any polynomials and we choose our learning parameter such that we expect an initial decreasing trend, we suggest polynomials of degree $4, 6$ or $8$ to be used to fit the data to find u-shaped trends.

Finally for the value of window length to detect that we have reached the minimum, we choose a value of $W$ such that the number of iterations in the window ($W \times I$) is big enough (around a hundred iterations) that we can confidently say the graph of the MSE error has reached a minimum value and started to increase in value (an increasing trend). Notice that the

33

window length should not be too big so that we can start the search in the local neighborhood and minimize the training time.

## References

Azimzadeh, P., Forsyth, P., 2015. The Existence of Optimal Bang-Bang Controls for GMxB Contracts. SIAM Journal on Financial Mathematics 6, 117–139.

Bishop, C.M., 2006. Pattern Recognition and Machine Learning (Information Science and Statistics). Springer-Verlag, NJ, USA.

Boyd, S., Vandenberghe, L., 2004. Convex Optimization. Cambridge University Press, NY, USA.

Boyle, P., Tian, W., 2008. The Design of Equity-Indexed Annuities. Insurance: Mathematics and Economics 43, 303–315.

Burrough, P., McDonnell, R., Lloyd, C., 1998. Principles of Geographical Information Systems. 2nd ed., Oxford University Press.

Belanger, A., Forsyth, P., Labahn, G., 2009. Valuing the Guaranteed Minimum Death Benefit Clause with Partial Withdrawals. Applied Mathematical Finance 16, 451–496.

Carriere, J., 1996. Valuation of the Early-Exercise Price for Options Using Simulations and Nonparametric Regression. Insurance: Mathematics and Economics 19, 19–30.

Cathcart, M., Morrison, S., 2009. Variable Annuity Economic Capital: the Least-Squares Monte Carlo Approach. Life & Pensions , 36–40.

Chen, Z., Forsyth, P., 2008. A Numerical Scheme for the Impulse Control Formulation of Pricing Variable Annuities with a Guaranteed Minimum Withdrawal Benefit (GMWB). Numerische Mathematik 109, 535–569.

Chen, Z., Vetzal, K., Forsyth, P., 2008. The Effect of Modelling Parameters on the Value of GMWB Guarantees. Insurance: Mathematics and Economics 43, 165–173.

Chi, Y., Lin, X.S., 2012. Are Flexible Premium Variable Annuities Underpriced? ASTIN Bulletin 42, 559–574.

Dai, M., Kwok, Y.K., Zong., J., 2008. Guaranteed Minimum Withdrawal Benefit in Variable Annuities. Journal of Mathematical Finance 18, 595–611.

Daul, S., Vidal, E., 2009. Replication of Insurance Liabilities. RiskMetrics Journal 9, 79–96.

Dembo, R., Rosen, D., 1999. The Practice of Portfolio Replication: A Practical Overview of Forward and Inverse Problems. Annals of Operations Research 85, 267–284.

Fox, J., 2013. A Nested Approach to Simulation VaR Using MoSes. Insights: Financial Modelling , 1–7.

Gan, G., 2013. Application of Data Clustering and Machine Learning in Variable Annuity Valuation. Insurance: Mathematics and Economics 53, 795–801.

Gan, G., Lin, X.S., 2015. Valuation of Large Variable Annuity Portfolios Under Nested Simulation: A Functional Data Approach. Insurance: Mathematics and Economics 62, 138–150.

Hardy, M., 2003. Investment Guarantees: Modeling and Risk Management for Equity-Linked Life Insurance. John Wiley & Sons, Inc., Hoboken, New Jersey.

Hejazi, S.A., Jackson, K.R., Gan, G., 2015. A Spatial Interpolation Framework for Efficient Valuation of Large Portfolios of Variable Annuities. URL: http://www.cs.toronto.edu/pub/reports/na/IME-Paper1.pdf.

Hornik, K., 1991. Approximation Capabilities of Multilayer Feedforward Networks. Neural Networks 4, 251–257.

Huang, Y., Forsyth, P., 2011. Analysis of a Penalty Method for Pricing a Guaranteed Minimum Withdrawal Benefit (GMWB). IMA Journal of Numerical Analysis 32, 320–351.

Hull, J.C., 2006. Options, Futures, and Other Derivatives. 6th ed., Pearson Prentice Hall, Upper Saddle River, NJ.

IRI, 2011. The 2011 IRI Fact Book. Insured Retirement Institute .

Longstaff, F., Schwartz, E., 2001. Valuing American Options by Simulation: A Simple Least-Squares Approach. The Review of Financial Studies 14, 113–147.

Milevsky, M., Salisbury, T., 2006. Financial Valuation of Guaranteed Minimum Withdrawal Benefits. Insurance: Mathematics and Economics 38, 21–38.

Moenig, T., Bauer, D., 2011. Revisiting the Risk-Neutral Approach to Optimal Policyholder Behavior: A Study of Withdrawal Guarantees in Variable Annuities, in: 12th Symposium on Finance, Banking, and Insurance, Germany.

Murphy, K.P., 2012. Machine Learning: A Probabilistic Perspective. The MIT Press.

Nadaraya, E.A., 1964. On Estimating Regression. Theory of Probability and its Applications 9, 141–142.

Nesterov, Y., 1983. A Method of Solving a Convex Programming Problem with Convergence Rate O(1/sqrt(k)). Soviet Mathematics Doklady 27, 372–376.

Nesterov, Y., 2003. Introductory Lectures on Convex Optimization: A Basic Course. Applied Optimization, Springer US.

Oechslin, J., Aubry, O., Aellig, M., Kappeli, A., Bronnimann, D., Tandonnet, A., Valois, G., 2007. Replicating Embedded Options in Life Insurance Policies. Life & Pensions , 47–52.

Polya, B.T., 1964. Some Methods of Speeding up the Convergence of Iteration Methods. USSR Computational Mathematics and Mathematical Physics 4, 1–17.

Reynolds, C., Man, S., 2008. Nested Stochastic Pricing: The Time Has Come. Product Matters!— Society of Actuaries 71, 16–20.

Sutskever, I., Martens, J., Dahl, G., Hinton, G., 2013. On The Importance of Initialization and Momentum in Deep Learning, in: Proceedings of the 30th International Conference on Machine Learning (ICML-13), JMLR Workshop and Conference Proceedings. pp. 1139–1147.

TGA, 2013. Variable Annuities—An Analysis of Financial Stability. The Geneva Association URL: `https://www.genevaassociation.org /media/ga2013/99582-variable-annuities.pdf`.

Ulm, E., 2006. The Effect of the Real Option to Transfer on the Value of Guaranteed Minimum Death Benefit. The Journal of Risk and Insurance 73, 43–69.

Vadiveloo, J., 2011. Replicated Stratified Sampling-a New Financial Modelling Option. Tower Watson Emphasis Magazine , 1–4.

Watson, G.S., 1964. Smooth Regression Analysis. Sankhyā: Indian Journal of Statistics 26, 359–372.